Article

Structure

Coiled-Coil Domains of SUN Proteins as Intrinsic Dynamic Regulators

Graphical Abstract

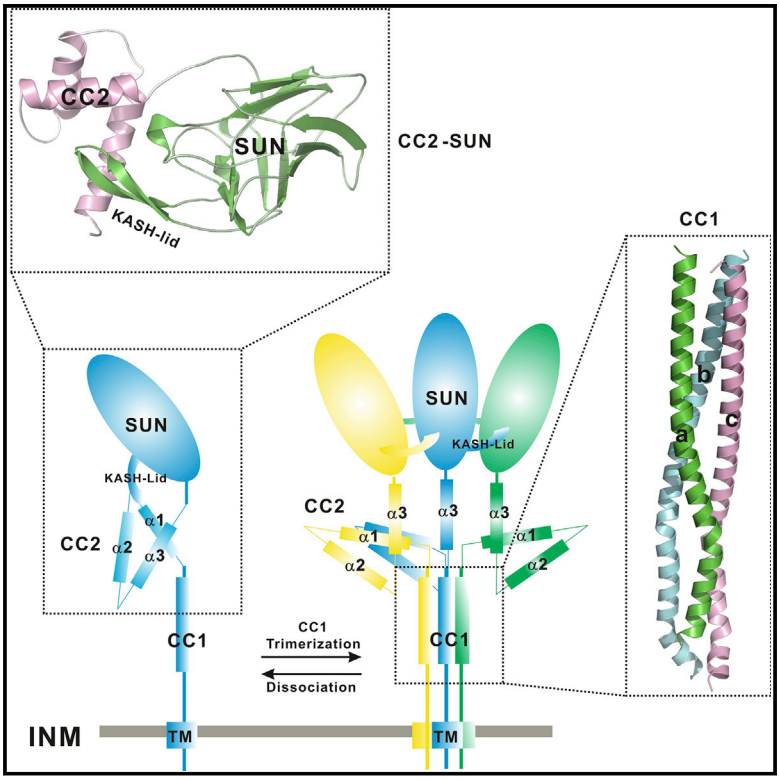

Authors

Si Nie, Huimin Ke, Feng Gao, ...,
Lin Huo, Weimin Gong, Wei Feng

Correspondence

wfeng@ibp.ac.cn

In Brief

SUN proteins contain at least one predicted coiled-coil domain preceding the SUN domain. Nie et al. determine the crystal structures of the different fragments including the coiled-coil and SUN domains from SUN2, which provide the molecular mechanism underlying the internal coiled-coil-mediated regulation of SUN proteins.

Highlights

- The two coiled-coil domains of SUN2 exhibit distinct oligomeric states
- CC2 forms a three-helix bundle to lock the SUN domain in an inactive conformation
- CC1 is a trimeric coiled coil for the trimerization and activation of the SUN domain
- The two coiled-coil domains of SUN2 act as the intrinsic dynamic regulators

Accession Numbers

5ED8
5ED9

Nie et al., 2016, Structure *24*, 80–91
January 5, 2016
http://dx.doi.org/10.1016/j.str.2015.10.024

CellPress

Structure
Article

Coiled-Coil Domains of SUN Proteins as Intrinsic Dynamic Regulators

Si Nie,[1,3] Huimin Ke,[1,3] Feng Gao,[2] Jinqi Ren,[1] Mingzhu Wang,[1] Lin Huo,[1] Weimin Gong,[2] and Wei Feng[1,*]
[1]National Laboratory of Biomacromolecules, Institute of Biophysics, Chinese Academy of Sciences, 15 Datun Road, Beijing 100101, China
[2]Laboratory of Non-coding RNA, Institute of Biophysics, Chinese Academy of Sciences, 15 Datun Road, Beijing 100101, China
[3]Co-first author
*Correspondence: wfeng@ibp.ac.cn
http://dx.doi.org/10.1016/j.str.2015.10.024

SUMMARY

SUN proteins are the core components of LINC complexes that span across the nuclear envelope for nuclear positioning and migration. SUN proteins contain at least one predicted coiled-coil domain preceding the SUN domain. Here, we found that the two coiled-coil domains (CC1 and CC2) of SUN2 exhibit distinct oligomeric states. CC2 is a monomer in solution. The structure of the CC2-SUN monomer revealed that CC2 unexpectedly folds as a three-helix bundle that interacts with the SUN domain and locks it in an inactive conformation. In contrast, CC1 is a trimer. The structure of the CC1 trimer demonstrated that CC1 is an imperfect coiled coil for the trimerization and activation of the SUN domain. Modulations of CC1 and CC2 dictate different oligomeric states of CC1-CC2-SUN, which is essential for LINC complex formation. Thus, the two coiled-coil domains of SUN2 act as the intrinsic dynamic regulators for controlling the SUN domain activity.

INTRODUCTION

The nuclear envelope (NE) is a double-membrane structure that includes the inner and outer nuclear membranes (INM and ONM, respectively), and serves as a physical barrier to partition the nuclear and cytoplasmic environments (Hetzer, 2010; Shimi et al., 2012; Wilson and Berk, 2010). More than 60 putative integral membrane proteins have been found to reside in either the INM or the ONM to decorate the NE and secure the structural integrity (Schirmer et al., 2003). Moreover, these NE-resident proteins often function together to form protein complexes that span across the NE and connect the nuclear lamina to the cytoskeleton, and thus are referred to as linkers of nucleoskeleton and cytoskeleton (LINC) (Razafsky and Hodzic, 2009; Starr and Fridolfsson, 2010).

LINC complexes are formed by coupling of KASH (Klarsicht, ANC-1, and Syne/Nesprin Homology) and SUN (Sad1 and UNC-84) proteins from the ONM and INM, respectively (Crisp et al., 2006). KASH proteins are featured with a single transmembrane helix and a short C-terminal tail penetrating the perinuclear space (together known as the KASH domain) (Starr and Fischer, 2005; Wilhelmsen et al., 2006). The N-terminal regions of KASH proteins are exposed in the cytoplasm, where they can associate with the cytoskeleton (Luxton and Starr, 2014; Mellad et al., 2011). SUN proteins harbor at least one transmembrane segment and a C-terminal family-specific SUN domain that can bind to the KASH domain within the lumen of the NE (Starr and Fridolfsson, 2010; Tzur et al., 2006). In contrast to KASH proteins, the N-terminal regions of SUN proteins are exposed in the nucleoplasm and contain signature motifs that are required for interacting with the nuclear lamina (Gruenbaum et al., 2005; Haque et al., 2006). Thus the formation of LINC complexes by KASH and SUN proteins at the NE establishes the physical linkage between the cytoskeleton and nuclear lamina, which is instrumental for the mechanical force transmission from the cytoplasm to the nuclear interior, and is essential for cellular processes such as nuclear positioning and migration, centrosome-nucleus anchorage, and chromosome dynamics (Burke and Roux, 2009; Chang et al., 2015; Hiraoka and Dernburg, 2009; Zhou and Hanna-Rose, 2010). In mammals, LINC complexes can be assembled by at least four KASH proteins (Syne/Nesprin-1 to -4) and two widely expressed SUN proteins (SUN1 and SUN2) (Mellad et al., 2011; Starr and Fridolfsson, 2010). Defects of these proteins are also related to a broad spectrum of muscle pathologies (e.g., Emery-Dreifuss muscular dystrophy and dilated cardiomyopathy) and neuronal disorders (such as lissencephalies) (Cartwright and Karakesisoglou, 2014; Fridkin et al., 2009; Mejat and Misteli, 2010).

Recognition between the SUN and KASH domains in the perinuclear space is pivotal for the formation of LINC complexes (Sosa et al., 2013; Tapley and Starr, 2013). Recent structural studies of the SUN domain of SUN2 demonstrated that it adopts a β-sandwich fold with a long flexible loop (namely, the KASH-lid) (Sosa et al., 2012; Zhou et al., 2012). A short segment preceding the SUN domain forms a parallel three-stranded coiled coil to drive the formation of a homo-trimer (Sosa et al., 2012). The structure of the LINC (SUN-KASH) complex further revealed that the flexible KASH-lid in the apo-SUN domain becomes well folded in the complex and forms a β hairpin, which intimately pairs with the KASH domain and anchors it in the protomer interfaces of the SUN domain homo-trimer (Sosa et al., 2012; Wang et al., 2012). In addition, the extreme C-terminal proline-rich tail of the KASH domain inserts into a tailor-made pocket within the SUN domain (Sosa et al., 2012). Thus, the extensive multivalent interactions between the SUN and KASH domains

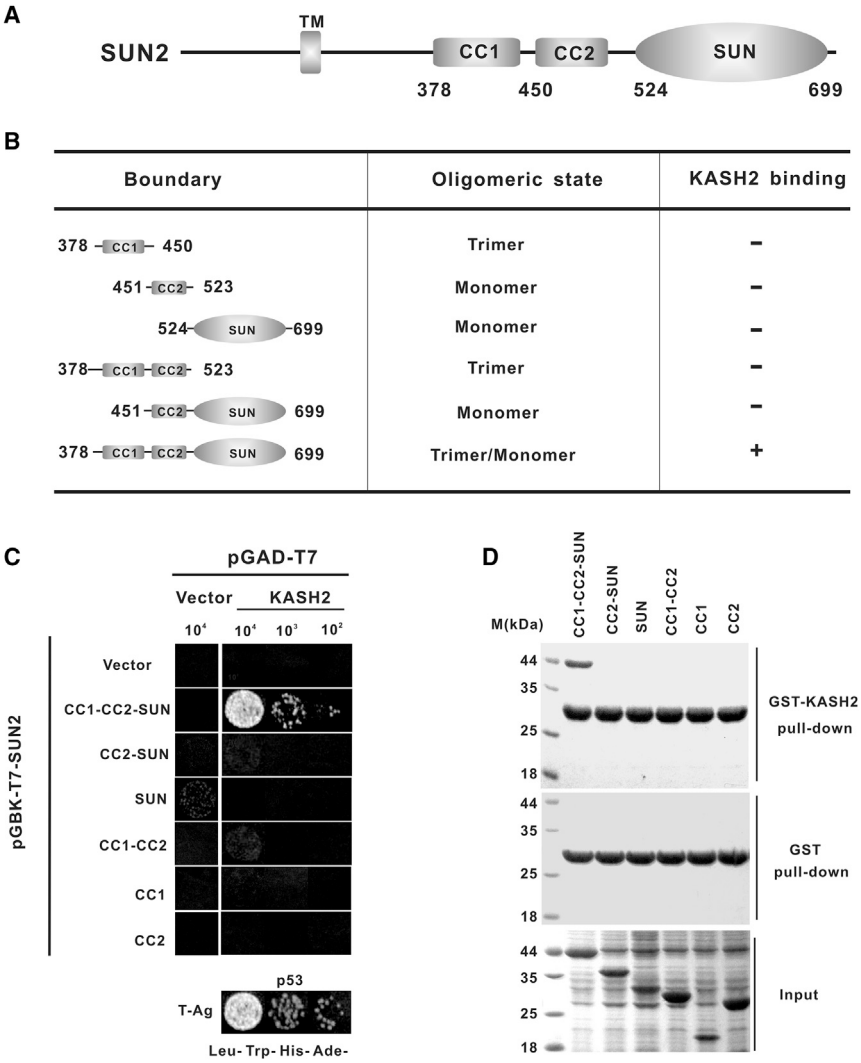

Figure 1. Biochemical Characterization of the Fragments Containing the Coiled-Coil and SUN Domains

(A) Domain organization of SUN2. SUN2 contains an N-terminal flexible region, a single transmembrane domain (TM), two coiled-coil domains (CC1 and CC2), and a C-terminal SUN domain.

(B) A summary of the biochemical data about the oligomeric states and KASH2-binding capacities of different SUN2 fragments. +, binding; −, no binding.

(C) Yeast-two-hybrid assay of the binding between different SUN2 fragments and the KASH2 peptide. The interaction between p53 and T-Ag was used as the positive control.

(D) In vitro GST pull-down assay of the interactions between different SUN2 fragments and the KASH2 peptide. The GST alone was used as the negative control.

See also Figures S1, S2, and S3.

ensure the formation of the stable hetero-hexameric SUN-KASH complex.

Besides the core SUN domain, SUN2 possesses two coiled-coil domains (CC1 and CC2) (predicted by COILS; Lupas et al., 1991) that precede the SUN domain and are predicted to be capable of oligomerization for homo-trimer assembly (Sosa et al., 2012) (Figure 1A). Moreover, these coiled-coil domains are also believed to act as rigid spacers to delineate the distance between the ONM and INM of the NE (Sosa et al., 2013). In addition to the functions predicted above, the two coiled-coil domains of SUN2 have been indicated to be able to directly modulate SUN domain activity and regulate the subsequent interactions between the SUN and KASH domains (Stewart-Hutchinson et al., 2008; Wang et al., 2012). It has been proposed that CC2 can inhibit the SUN domain, while CC1 functions as an activation segment to release CC2-mediated inhibition (Wang et al., 2012). Thus, the coiled-coil domains of SUN2 may not simply function as passive linear coiled coils for oligomerization but are actively involved in controlling the target-binding capacity of the SUN domain. However, the molecular mechanism underlying the internal coiled-coil-mediated regulation of the SUN domain is poorly understood.

In this study, we characterized the two coiled-coil domains of SUN2 and found that they exhibit two distinct oligomeric states, i.e., CC1 forms a trimer but CC2 is a monomer. We determined the crystal structures of the CC2-SUN monomer and the CC1 trimer. In the CC2-SUN monomer, CC2 folds as a three-helix bundle that tethers the SUN domain and locks it in an inactive conformation. In the CC1 trimer, CC1 forms an imperfect trimeric coiled coil that can induce the trimerization and activation of the SUN domain. Modulations of CC1 and CC2 dictate different oligomeric states of CC1-CC2-SUN and the subsequent interaction with the KASH domain. Thus, CC1 and CC2 of SUN2 play diverse roles in the regulation of SUN domain activity.

RESULTS

The Two Coiled-Coil Domains of SUN2 Exhibit Distinct Oligomeric States

Since the two coiled-coil domains of SUN2 have been indicated in the regulation of the SUN domain (Wang et al., 2012), we initiated this study by the biochemical characterization of the two coiled-coil domains and various fragments containing the coiled-coil and SUN domains using analytic gel filtration, chemical cross-linking, and size-exclusion chromatography (SEC) coupled with multi-angle light scattering assays (Figures 1A, 1B, S1, and S2). We also evaluated the direct binding between these fragments and the C-terminal peptide from the KASH domain of Nesprin-2 (the KASH2 peptide) by yeast-two-hybrid assay and GST pull-down experiments (Figures 1C and 1D). Unexpectedly, the two coiled-coil domains of SUN2 exist in two different oligomeric states, i.e., CC1 forms a trimer but CC2 is a monomer, although neither of

Table 1. Data Collection and Refinement Statistics

Data Collection				
Dataset	Native-CC2-SUN	Se-Met-CC2-SUN	Se-Met-CC1-CC2	Native-CC1
Space group	$P4_12_12$	$P4_12_12$	$P2_1$	$C2$
Unit cell parameters				
a, *b*, *c* (Å)	64.4, 64.4, 192.8	63.9, 63.9, 194.1	61.3, 35.2, 75.8	86.4, 34.7, 99.8
α, β, γ (°)	90, 90, 90	90, 90, 90	90, 105.4, 90	90, 101.5, 90
Resolution range (Å)	50–2.5 (2.59–2.5)	50–2.8 (2.9–2.8)	50–2.0 (2.03–2.0)	50–2.0 (2.07–2.0)
No. of total reflections	62,509 (6,232)	215,477 (21,693)	21,492 (1,062)	19,246 (1867)
No. of unique reflections	14,373 (1,385)	10,703 (1,033)	2,944 (143)	3,564 (352)
I/σ	21.6 (2.4)	21.9 (11.3)	11.7 (2.5)	9.1 (3.4)
Completeness (%)	99.5 (100)	99.7 (100.0)	99.3 (100.0)	98.6 (97.9)
R_{merge} (%)[a]	6.9 (53.2)	12.6 (44.6)	11.6 (94.7)	16.3 (58.0)
Structure Refinement				
Resolution (Å)	32.94–2.50 (2.59–2.50)			36–2.0 (2.1–2.0)
R_{cryst}/R_{free} (%)[b]	21.3 (29.8)/25.4 (35.3)			21.1 (19.9)/25.7 (26.5)
Average *B* factors (Å^2)	80.1			33.0
Root-mean-square deviation bonds (Å)/angles (°)	0.003/0.766			0.005/0.823
Ramachandran plot				
Favored regions (%)	93.1			99.5
Allowed regions (%)	6.9			0.5
Disallowed (%)	0.0			0.0

$R_{free} = \Sigma_T||F_{obs}| - |F_{calc}||/\Sigma_T|F_{obs}|$, where T is a test dataset of about 5% of the total reflections randomly chosen and set aside prior to refinement. Numbers in parentheses represent the value for the highest-resolution shell.

[a]$R_{merge} = \sum|I_i - I_m|/\sum I_i$, where I_i is the intensity of the measured reflection and I_m is the mean intensity of all symmetry-related reflections.

[b]$R_{cryst} = \Sigma||F_{obs}| - |F_{calc}||/\Sigma|F_{obs}|$, where F_{obs} and F_{calc} are observed and calculated structure factors.

them can bind to the KASH2 peptide (Figures 1B–1D, S1, and S2). As the control, the SUN domain alone adopts a monomeric conformation without the KASH2 peptide-binding capacity (Figures 1B–1D), consistent with previous studies (Sosa et al., 2012). The covalent linkage of CC2 and the SUN domain resulted in the CC2-SUN fragment that still exists in a monomeric state and is unable to interact with the KASH2 peptide (Figures 1B–1D), indicating that CC2 is unlikely to be a proposed trimeric coiled coil for SUN domain activation. Consistently, CC2 is largely α-helical in solution (with a 222-/208-nm ratio of 0.82 in circular dichroism [CD] analysis) and CC1 predominantly forms coiled coils (with 222-/208-nm ratio of 1.01) (Kwok and Hodges, 2004) (Figure S3). In contrast, the further extension of CC2-SUN to CC1 induced the trimerization and activation of the SUN domain, since the resulting CC1-CC2-SUN fragment shows a large fraction of trimeric components and can bind to the KASH2 peptide (Figures 1B–1D). Thus, consistent with previous studies (Wang et al., 2012), distal CC1 (with respect to the SUN domain) is most likely the predominant trimerization and activation site for the SUN domain, while proximal CC2 is not. Moreover, CC1-CC2 adopts a trimeric state but CC1-CC2-SUN exists in a monomer-trimer equilibrium (rather than a homogeneous trimer) (Figures 1B, S1, and S2), suggesting the potential interactions between the coiled-coil and SUN domains that could interfere with the trimeric conformation of CC1-CC2-SUN (see below for details).

Overall Structure of the CC2-SUN Monomer

To uncover the molecular mechanism underlying the coiled-coil-mediated regulation of the SUN domain, we next performed crystal screening of CC2-SUN and CC1-CC2-SUN. After extensive trials, we achieved high-quality crystals of CC2-SUN but not CC1-CC2-SUN (possibly due to its heterogeneous state; Figures S1 and S2). The crystal structure of CC2-SUN was solved by the single-wavelength anomalous dispersion method and was refined to 2.5 Å resolution (Table 1). Consistent with the biochemical characterizations, only one CC2-SUN molecule was found in the asymmetric unit. In this monomer structure, the SUN domain is composed of 12 β strands (β1–β12) and three 3_{10} helices (η1–η3), which are arranged into a dual-sheet β sandwich (Figure 2A). The KASH-lid (a β-hairpin structure formed by antiparallel β2 and β3) and η3 of the SUN domain protrude from the β-sandwich base, together with β4, β11, and the η2/β4 loop, to construct a deep pocket (Figure 2A), which serves as a specific site for binding to the C-terminal proline-rich tail of the KASH domain (Sosa et al., 2012).

As expected, instead of forming an extended coiled coil, CC2 is broken into three short α helices (α1–α3) that form a partially open three-helix bundle in this CC2-SUN structure (Figure 2A), consistent with the CD analysis (Figure S3). In the crystal packing of the CC2-SUN structure, no obvious artificial contacts from the neighboring molecules were found to influence the three-helix bundle structure of CC2 (Figure S4). More significantly, consistent with the above assumption about the coiled-coil/SUN

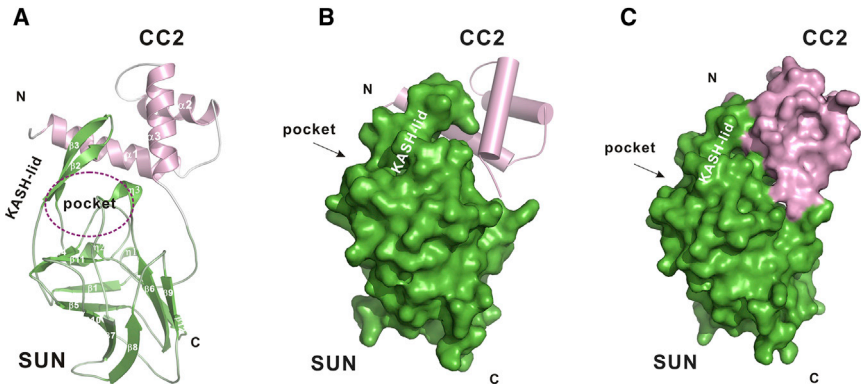

Figure 2. Overall Structure of the CC2-SUN Monomer

(A) A ribbon diagram of the structure of CC2-SUN. The SUN domain and CC2 are colored in green and pink, respectively. The secondary structures of CC2-SUN are labeled, and both N and C termini are also marked.

(B) A combined surface and ribbon representation of the CC2-SUN monomer structure. The SUN domain is in the surface representation (colored green), and CC2 is in the ribbon representation (colored pink).

(C) A surface representation of CC2-SUN showing that the SUN domain and CC2 pack extensively with each other to form one structural unit. The SUN domain and CC2 are colored as in (A).

See also Figure S4.

domain interactions, this three-helix bundle further makes extensive contacts with the SUN domain, i.e., the KASH-lid of the SUN domain directly inserts into the packing core of the CC2 three-helix bundle, which would most likely complete this partially open three-helix bundle (Figure 2B). Thus, the structure of the CC2-SUN monomer demonstrated that CC2 and the SUN domain are not independent but can be integrated by the KASH-lid to form one compact structural unit with a kidney-bean-like shape (Figure 2C).

The Inter-domain Interaction Interface within the Compact CC2-SUN Structure

The inter-domain interaction interface between CC2 and the SUN domain is mediated by the KASH-lid and η3 of the SUN domain and the open site of the CC2 three-helix bundle (Figure 3A). In the CC2 three-helix bundle, α3 packs with α2 and the C-terminal end of α1, and the inter-helical packing can be separated into two hydrophobic clusters, i.e., one is constructed by L493, I496, and L497 from α2, V510 and I513 from α3, and V505 from the α2/α3 loop, and the other is formed by M478 from α1, A489 from α2, M481 from the α1/α2 loop, and V514, A517, and L518 from α3 (Figures 3C and S5). However, the N-terminal part of α1 is not involved in the inter-helical packing of the three-helix bundle but is completely exposed to interact with the KASH-lid of the SUN domain. More specifically, L558, F559, I561, and L563 from the KASH-lid form hydrophobic contacts with L467, L470, and I474 from α1 (Figures 3B and S5). A small cluster of hydrogen-bonding/electrostatic interactions is formed by Y565 from the KASH-lid, E471 from α1, and R520 from α3, which would stabilize the inter-domain packing between the KASH-lid and α1 (Figure 3B). In addition to these interactions, the KASH-lid is close to the η2/β4 loop and η3 that further make contacts with the C-terminal ends of both α1 and α3 (Figure 3B). Taken together, the intimate packing between CC2 and the SUN domain integrates the two domains to form a compact monomer.

The SUN Domain Adopts an Inactive Conformation in the CC2-SUN Monomer

The structure of the hetero-hexameric SUN-KASH complex revealed that the trimerization of the SUN domain, predominantly mediated by the short helix α3 of CC2, is prerequisite for binding to the KASH domain (Figure 4A). However, in the CC2-SUN structure, the helix α3 acts as the central component of the CC2 three-helix bundle and is unable to promote the SUN domain trimerization (Figures 4B and 4C). Moreover, the KASH-lid of the SUN domain that is essential for pairing with the KASH domain is directly captured by the CC2 three-helix bundle (Figure 4B). Thus, in the CC2-SUN monomer, the SUN domain is tightly tethered by CC2 and is most likely locked in an inactive state. Consistent with this structural feature, the CC2-SUN monomer showed no capacity for binding to the KASH2 peptide (Figures 1C and 1D).

To further dissect the inactive SUN domain in the CC2-SUN monomer, we compared the structure of CC2-SUN with that of the SUN-KASH complex by superimposing the two essentially similar β sandwiches (Figure 4B). Besides the obvious oligomeric state change of α3, the KASH-lid of the SUN domain undergoes significant conformational changes (Figures 4C and 4D). More specifically, the KASH-lid in CC2-SUN bears a rotation of ~90° clockwise toward the CC2 three-helix bundle and resembles a pair of fingers grasping one edge of this three-helix bundle (Figures 4B and 4D). In addition to the lateral rotation, the two sides of the KASH-lid flip over, i.e., W564, L556, and A554 facing inside in the SUN-KASH complex flip outside in CC2-SUN, while Y565, L555, and S557 flip oppositely (Figure 4D). Thus, the KASH-lid of the SUN domain is likely to transit from a straight, open conformation in the SUN-KASH complex to a twisted, closed form in the CC2-SUN monomer.

Disruptions of the CC2 Three-Helix Bundle Restore the KASH-Binding Capacity of the SUN Domain

Since the CC2 three-helix bundle sequesters the KASH-lid of the SUN domain in CC2-SUN (Figure 3A), we predicted that disruptions of this three-helix bundle would release the KASH-lid and concomitantly expose α3 to mediate SUN domain trimerization for binding to the KASH domain. To validate this hypothesis, we made a series of mutations in CC2 to disassemble the three-helix bundle, and evaluated the interactions between these CC2-SUN mutants and the KASH2 peptide (Figures 3D and 3E). As α3 is the essential component in the SUN-KASH complex structure (Figure 4A), we did not make mutations in this segment but only in α1 and α2, e.g., deletion of α1 (Δα1) or of α1 and α2 (Δα1/α2), or substitution of hydrophobic residues with hydrophilic ones in α1 (I474Q/M478Q) or α2 (I496Q/L497Q). As expected, compared with

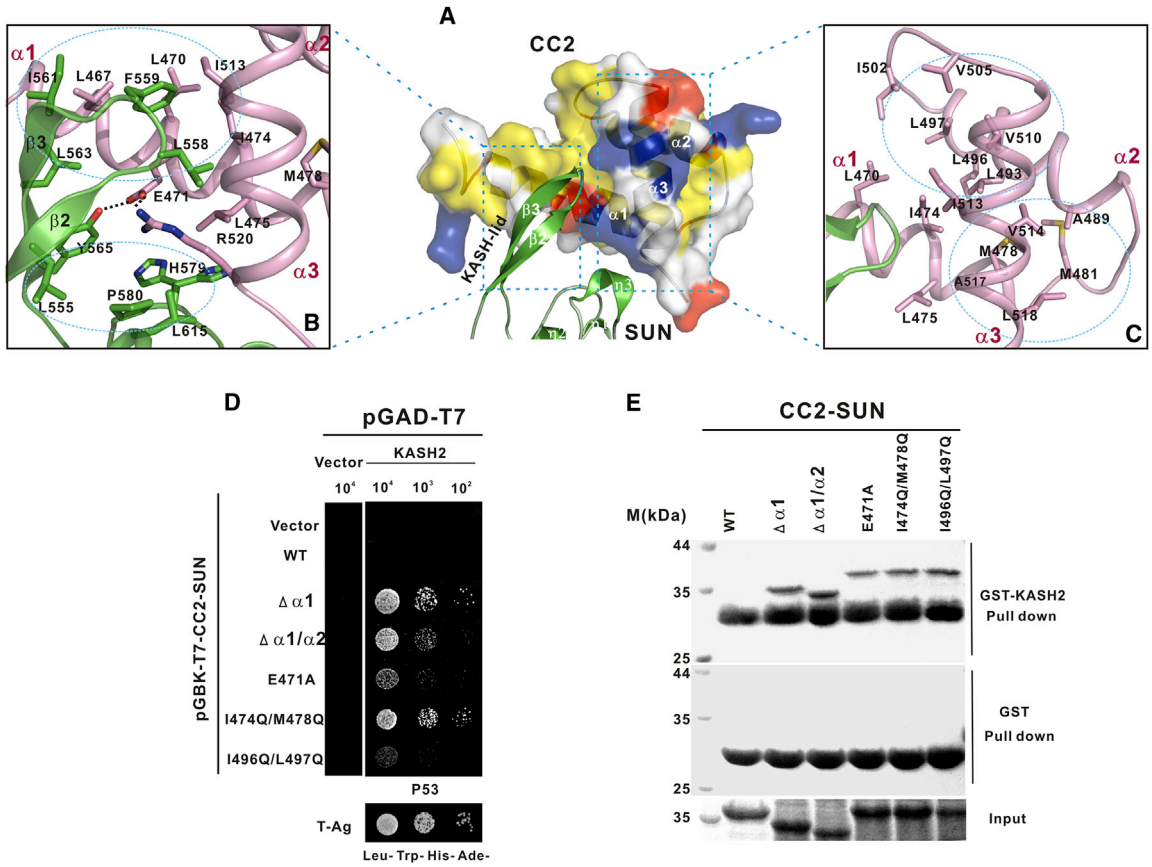

Figure 3. Inter-domain Interaction Interface in the CC2-SUN Structure

(A) A combined surface and ribbon representation showing the inter-domain packing interfaces between CC2 and the SUN domain. The SUN domain is in the ribbon representation (colored green), and CC2 is in the surface representation. In this surface drawing, the hydrophobic, positively charged, negatively charged, and remaining residues are colored yellow, blue, red, and white, respectively.

(B) A combined ribbon and stick model illustrates the inter-domain interaction interface between the CC2 three-helix bundle and the SUN domain. In this drawing, CC2 and the SUN domain are colored pink and green, respectively, and the side chains of the residues involved in the inter-domain packing are shown as sticks.

(C) A combined ribbon and stick model illustrates the inter-helical packing interface between the CC2 three-helix bundle. The side chains of the residues involved in the inter-helical packing are shown as sticks.

(D) Yeast two-hybrid assay of the interactions between the CC2-SUN mutants and the KASH2 peptide. The interaction between p53 and T-Ag was used as the positive control.

(E) In vitro GST pull-down analysis of the interactions between the CC2-SUN mutants and the KASH2 peptide. The GST alone was used as the negative control. See also Figures S5 and S6.

wild-type CC2-SUN, all the CC2-defective mutants could bind to the KASH2 peptide (Figures 3D and 3E). Consistently, the CC2-SUN mutant with deletion of α1 and α2 is a mixture of trimer and monomer in solution (Figure S6), which was also observed in previous studies (Zhou et al., 2012). Given that the hydrogen-bonding/electrostatic interaction network (formed by E471, R520, and Y565) seems to bridge α1, α3, and the KASH-lid together (Figure 3B), we further made the E471A mutation in α1. Interestingly, this mutant could bind to the KASH2 peptide (Figures 3D and 3E), indicating that the hydrogen-bonding/charge interaction network is also essential for the inactive conformation of the SUN domain. Taken together, CC2 is the key factor in holding the inactive SUN domain in CC2-SUN, and the disassembly of the CC2 three-helix bundle can restore the KASH-binding capacity of the SUN domain.

Crystal Structure of the CC1 Trimer

Given that CC1 functions as the predominant site for SUN domain trimerization (rather than CC2) (Figure 1), we next investigated the mechanism underlying the CC1-mediated trimerization. We performed crystal screening of CC1 and CC1-CC2, since both of them adopt a trimeric state and form coiled coils in solution (Figures S2 and S3). Fortunately, the two CC1-containing fragments could both be crystallized, and we first focused on the longer fragment CC1-CC2 (Table 1). However, upon processing the diffraction data of CC1-CC2, we could only reasonably trace the electron density of CC1 but not that of CC2, possibly due to the intrinsic flexibility of CC2 (upon dissociation from the SUN domain) (Figure 2, and see Discussion). Thus, we failed in our initial attempt to solve the structure of CC1-CC2 and thus resorted to CC1 alone. Nevertheless, based on all the efforts with CC1-CC2, we determined the crystal

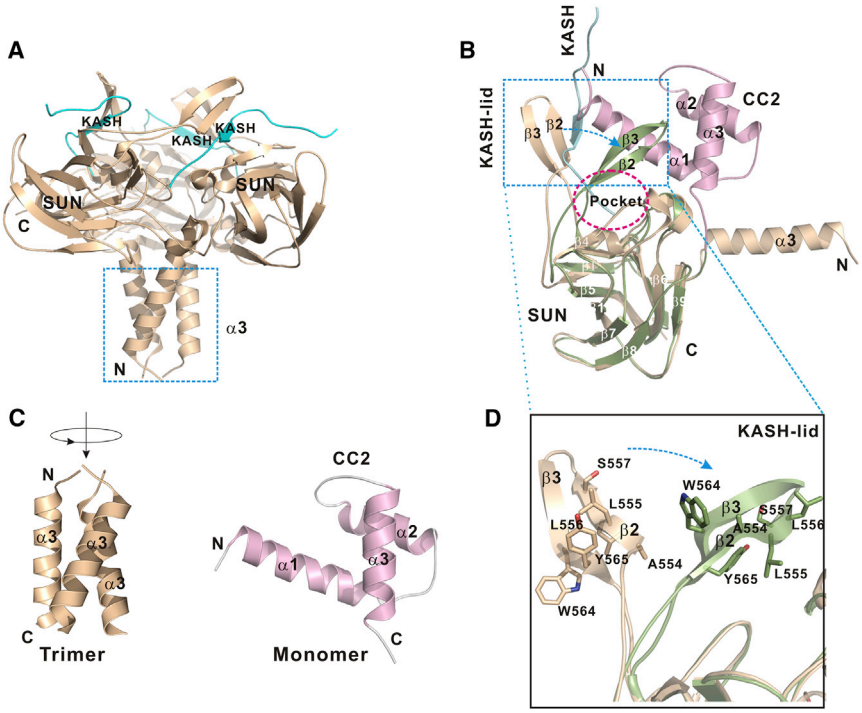

Figure 4. Structural Comparison of CC2-SUN with the SUN-KASH Complex

(A) A ribbon diagram of the structure of the SUN-KASH complex (PDB: 4DXS). The SUN domain and the KASH peptide are colored wheat and cyan, respectively.

(B) A ribbon diagram of CC2-SUN and the SUN-KASH complex by superimposing the central β-sandwich fold. CC2 and the SUN domain of CC2-SUN are colored pink and green, respectively, and one subunit of the SUN-KASH complex are colored as in (A).

(C) A ribbon diagram of the helix α3 from the SUN-KASH complex and the CC2 three-helix bundle.

(D) A combined ribbon and stick model illustrates the conformational changes of the KASH-lid in detail. The side chains of the residues involved in the flipping are shown as sticks.

structure of CC1 by the molecular replacement method to 2.0 Å resolution (Table 1). As expected, in this structure CC1 forms a parallel elongated trimeric coiled coil (αCC1a-αCC1c) that could promote SUN domain trimerization (Figure 5A). The three CC1 subunits from the parallel coiled-coil trimer are essentially the same except for the extreme C-terminal end, i.e., several C-terminal residues of one subunit are missing, possibly due to the intrinsic flexibility of the terminal end (Figure 5C). More significantly, the CC1 helix is not perfectly linear for the trimeric coiled-coil formation but possesses an obvious kink in the middle (Figure 5C). From the overall structure, this kink would induce the switch of the coiled-coil stacking within the CC1 trimer from a conventional "left-handed" to an unconventional "right-handed" pattern (Figure 5A).

Inter-helical Packing between the CC1 Coiled-Coil Trimer

The inter-helical interaction interface of the CC1 coiled-coil trimer is formed by the hydrophobic packing between the three helices (Figure 5B). Based on the heptad repeat pattern (*a*–*g*) analysis, the *a* and *d* positions of CC1 are mostly occupied by hydrophobic leucine residues (i.e., L394, L387, L400, L403, L407, L410, and L423) that are directly involved in the inter-helical packing (Figure 6A). However, in contrast to the classical hydrophobic packing, a number of unusual inter-helical packing features were found in the CC1 coiled-coil trimer. Firstly, some *a* and *d* positions of CC1 that are buried in the inter-helical interfaces are occupied by hydrophilic residues (such as S389 and Q414) (Figure 6A), which would destabilize the coiled-coil trimer. Secondly, CC1 contains two proline residues within the C-terminal half (P425 and P440), which would drive the formation of the kinks and distort the coiled-coil structure (Figures 5A and 6A). Finally, in addition to the aforementioned defects in the CC1 coiled-coil trimer, the coiled-coil stacking at the two termini is also irregular, i.e., both terminal ends contain a "stutter" break with the "3-4-4-3" pattern (versus the classical "3-4-3-4" pattern, the number indicating the interval of packing residues in the inter-helical interface) (Brown et al., 1996; Gruber and Lupas, 2003) (Figures 5D and 6A). Taken together, the above unusual packing features of CC1 indicate that it is not ideally designed for stable trimerization.

Modulations of CC1 and CC2 Dictate Different Oligomeric States of CC1-CC2-SUN

The above structural analysis of the CC1 trimer revealed the defects of this coiled-coil domain for trimerization (Figure 6A), consistent with the fact that CC1-CC2-SUN exists in a monomer-trimer equilibrium (rather than adopting a stable trimeric state,) possibly due to the intrinsic imperfection of CC1 (Figures S1 and S2). To further validate this hypothesis, two types of mutations in CC1 were made: one is the Q414L mutation that substitutes the hydrophilic residue in the inter-helical packing interface to stabilize the trimer, while the other is the L400A/L403A mutation that further destabilizes this trimeric coiled coil (Figure 6A). As expected, the Q414L mutation stabilized both CC1 and CC1-CC2, while the L400A/L403A mutation disrupted and destabilized the coiled-coil structures of CC1 and CC1-CC2 (Figure S3). Moreover, the monomer-trimer equilibrium of CC1-CC2-SUN was disrupted by these mutations, i.e., the Q414L mutant forms a stable trimer but the L400A/L403A mutant is a monomer (Figure 6B), indicating that the stabilization and destabilization of the CC1 coiled-coil trimer modulate the oligomeric states of CC1-CC2-SUN. On the other hand, the monomer-trimer equilibrium of CC1-CC2-SUN may also be caused by the interactions between CC2 and the SUN domain in addition to the defects of CC1, since CC1-CC2 is a trimer but CC2-SUN forms a compact monomer (Figures 1 and 2). To further test this assumption, we also made mutations in CC2 (Δα1, Δα2, I474Q/M478Q, and I496Q/L497Q) of CC1-CC2-SUN to disrupt the CC2/SUN domain interactions (Figure 3). All of these CC2-defective mutants exist in the trimeric state (Figure S7), suggesting

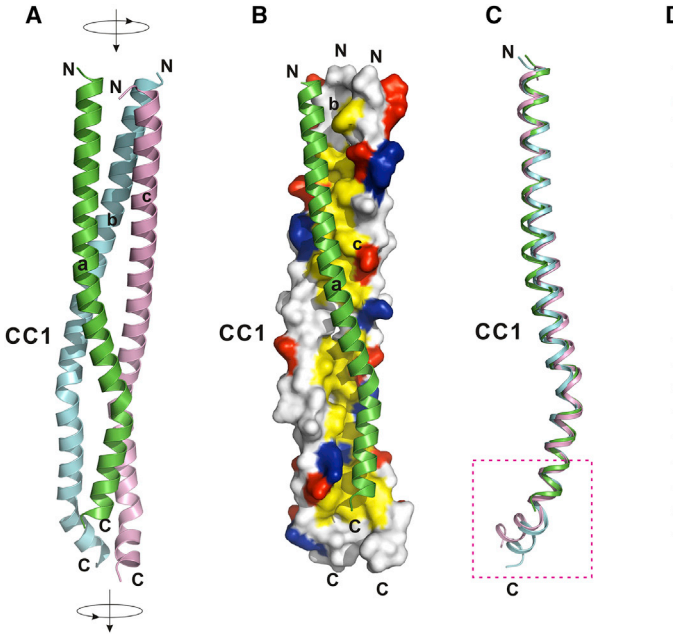

Figure 5. Structure of the CC1 Coiled-Coil Trimer

(A) A ribbon diagram of the structure of the CC1 trimer. The three helical subunits of CC1 are colored green, cyan, and pink, respectively.

(B) A combined surface and ribbon representation of the CC1 coiled-coil structure. One subunit of CC1 is in ribbon representation (colored green), and the other two subunits are in surface representation. In this surface drawing, the color scheme follows that of Figure 3A.

(C) Superposition of the three subunits of the CC1 coiled-coil trimer.

(D) The heptad repeat register of the residues for the coiled-coil packing of the CC1 trimer. The CC1 helix has been cut and opened flat to give a 2D representation. The hydrophobic residues and hydrophilic residues in the packing core are highlighted by yellow and red circles, respectively. Every seventh residue is repeated on the right of the plot (in parentheses).

that the interactions between CC2 and the SUN domain also contribute to the monomer-trimer equilibrium of CC1-CC2-SUN. Taken together, the monomer-trimer equilibrium of CC1-CC2-SUN is mediated by CC1 and CC2, and the modulations of these two coiled-coil domains can convert CC1-CC2-SUN between different oligomeric states.

The Coiled-Coil Domains of SUN2 Are Essential for SUN-KASH Complex Formation

All of the above data demonstrated that the coiled-coil domains of SUN2 are the regulatory sites for the SUN domain (Figures 5 and 6). To further probe the role of CC1 for the interactions between the SUN and KASH domains, we evaluated the binding between the different CC1-CC2-SUN mutants (with the mutations in the CC1 to stabilize or destabilize the trimer) and the KASH2 peptide. As expected, the Q414L mutant could directly interact with the KASH2 peptide while the L400A/L403A mutant could not (Figures 6C and 6D), indicating that the CC1 coiled-coil trimer is essential for the SUN-KASH interaction. To investigate the role of CC1 for SUN-KASH complex formation in vivo, we co-expressed SUN2 (with or without mutations in CC1) and KASH2 in HeLa cells and evaluated the cellular localization of the two proteins. KASH2 used in this study is a truncated form of Nesprin-2 that contains the transmembrane helix and the KASH domain (the mini-Nesprin-2 protein). As expected, KASH2 alone formed large clusters and could not be well localized to the NE (Figures 7A and 7B). Upon co-expression of SUN2, KASH2 could be localized to the NE (Figures 7A and 7B), suggesting that the localization of KASH2 to the NE largely depends on the interactions with SUN2, which is consistent with the findings of previous studies (Ostlund et al., 2009). The co-localizations of SUN2 and KASH2 at the NE also indicated formation of the SUN-KASH complex in the cells. Consistent with these binding data, in comparison with wild-type SUN2, the Q414L mutant induced more localizations of KASH2 to the NE while the L400A/L403A mutant did not (Figures 7A and 7B), indicating that the modulations of the CC1 coiled-coil trimer indeed affect SUN-KASH complex formation in vivo. To further evaluate the role of CC2 in SUN-KASH complex formation, we introduced the CC2 mutations in SUN2 and its CC1 loss-of-function mutant (the L400A/L403A mutant). As expected, the mutations (Δα1 and E471A) in CC2 slightly induced more localizations of KASH2 to the NE (Figures 7A and 7B), suggesting that these CC2-based mutants are active for binding to KASH2. Although the mutations of CC2 could somewhat rescue the defect of the CC1 loss-of-function mutant, these CC1/CC2 mutants still could not restore the NE localizations of KASH2 as efficiently as wild-type SUN2 (Figures 7A and 7B), indicating that the CC1-mediated trimerization of SUN2 is predominantly required for interacting with KASH2. In contrast, all of the mutations in CC1 and CC2 had minimum effects on the cellular localization of SUN2 (Figures 7A and 7B). Taken together, the biochemical and cellular data demonstrated that CC1 and CC2 are the essential sites of SUN2 for regulating the assembly of the SUN-KASH complex.

DISCUSSION

LINC (SUN-KASH) complexes formed by SUN and KASH proteins span across the NE and play fundamental roles in regulating various NE-related biological processes (Sosa et al., 2013; Starr and Fridolfsson, 2010). In addition to the SUN domain that can recognize the KASH domain, SUN proteins contain the predicted coiled-coil domains that are presumably able to form the trimeric coiled coil for promoting SUN domain trimerization, which is essential for LINC complex formation (Figure 1A). Here, we demonstrated that the two coiled-coil domains (CC1 and CC2) of SUN2 are not solely linear coiled coils for oligomerization but also act as active regulators in controlling SUN domain activity, which would be a significant advance in understanding the mechanism of internal coiled-coil-mediated regulation of SUN proteins.

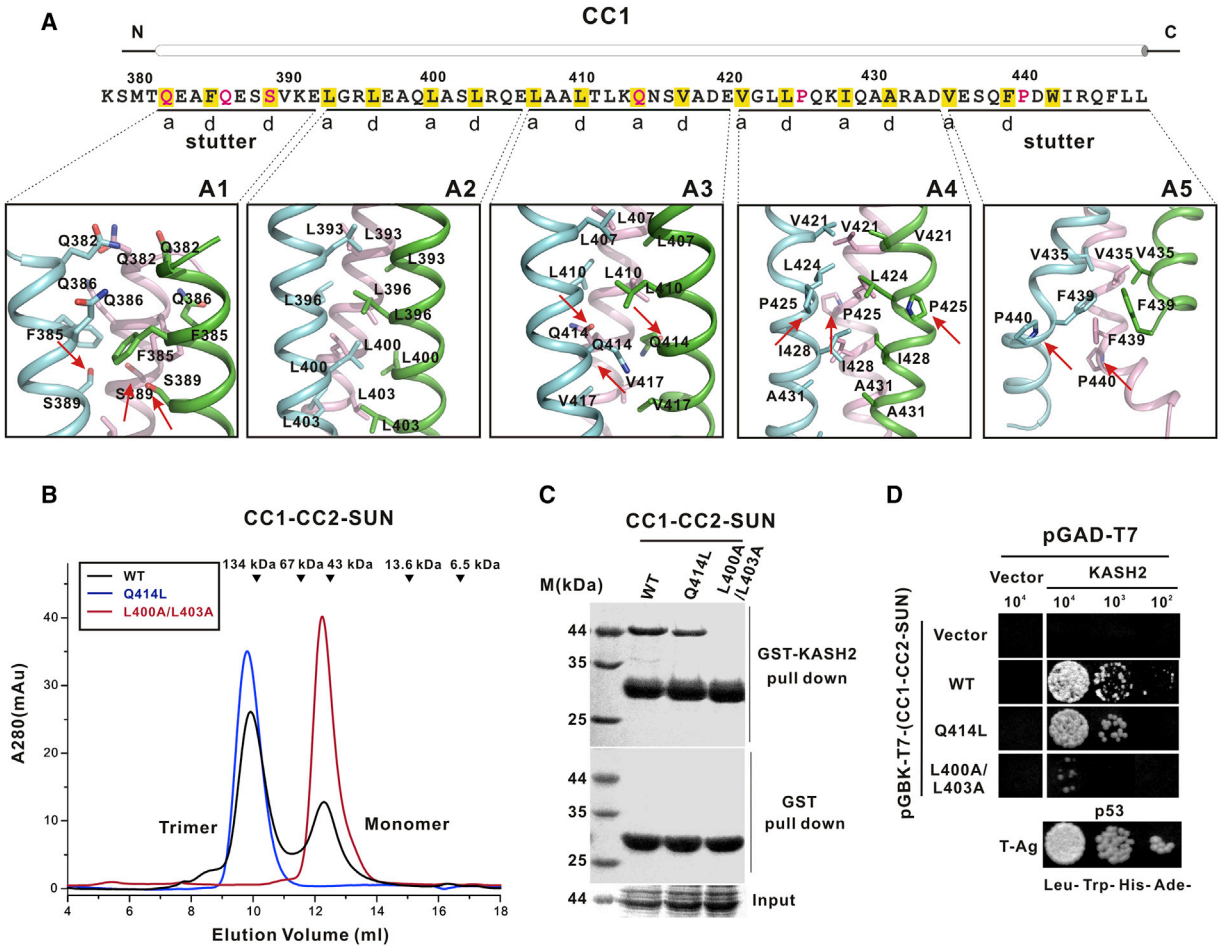

Figure 6. Inter-helical Packing Interface between the CC1 Coiled-Coil Trimer

(A) A combined ribbon and stick model illustrates the inter-helical packing interface between the CC1 trimer (A1–A5). The three helical subunits of CC1 are colored as in Figure 5A, and the residues involved in the inter-domain packing are shown as sticks. The residues that are likely to destabilize the coiled-coil formation are highlighted by red arrows. The sequence and secondary structure of CC1 are marked at the top of the panel. The *a* and *d* sites of CC1 for the inter-helical packing are also marked.

(B) Analytical gel-filtration analysis of the CC1-CC2-SUN mutants. The elution volumes of molecular weight markers are indicated at the top.

(C and D) GST pull-down analysis (C) and yeast-two-hybrid assay (D) of the interactions between the CC1-CC2-SUN mutants and the KASH2 peptide. All binding data are presented as shown in Figures 3D and 3E.

See also Figures S5 and S7.

CC2-Mediated Closed Conformation of the SUN Domain

Instead of forming a trimeric coiled coil, CC2 of SUN2 forms a three-helix bundle in the CC2-SUN structure (Figure 2). Structure-based sequence analysis demonstrated that several Gly residues are located in the flexible linker regions between the three helices (Figure S5), which would ideally provide the breaks/turns in CC2 for three-helix bundle formation. Thus, CC2 tends to be broken into short helices (α1–α3) instead of being a classical coiled coil (as predicted by COILS). More interestingly, the last helix α3 of CC2 (that is immediately connected to the SUN domain) has been shown to be an essential segment for promoting SUN domain trimerization in the SUN-KASH complex structure (Sosa et al., 2012; Wang et al., 2012) (Figure 4). Consistent with the essential role of α3, the CC2-SUN mutants were able to bind to the KASH2 peptide only with the deletion or disruption of α1 and α2, but not α3 (Figure 3). However, in the CC2-SUN monomer structure, helix α3 extensively packs with the other two helices and is unable to work together with the SUN domain (Figure 2). In addition, the KASH-lid of the SUN domain that is essential for anchoring the KASH domain in the SUN-KASH complex is also sequestered by CC2 (Figure 4). Thus, CC2 of SUN2 most likely acts as an inhibitory component that tethers the SUN domain and locks it in a closed inactive conformation (Figure 2). Consistent with this structural feature, both previous studies and our biochemical data of SUN2 demonstrated that the fragment including CC2 and the SUN domain is unable to bind to the KASH2 peptide (Stewart-Hutchinson et al., 2008; Wang et al., 2012) (Figure 1).

In the CC2-SUN structure, it is of interest to note that the CC2 three-helix bundle adopts a partially open conformation (Figures 2 and 4), indicating that this three-helix bundle is not stable. Consistently, CC2 and its mutants were intolerant of high

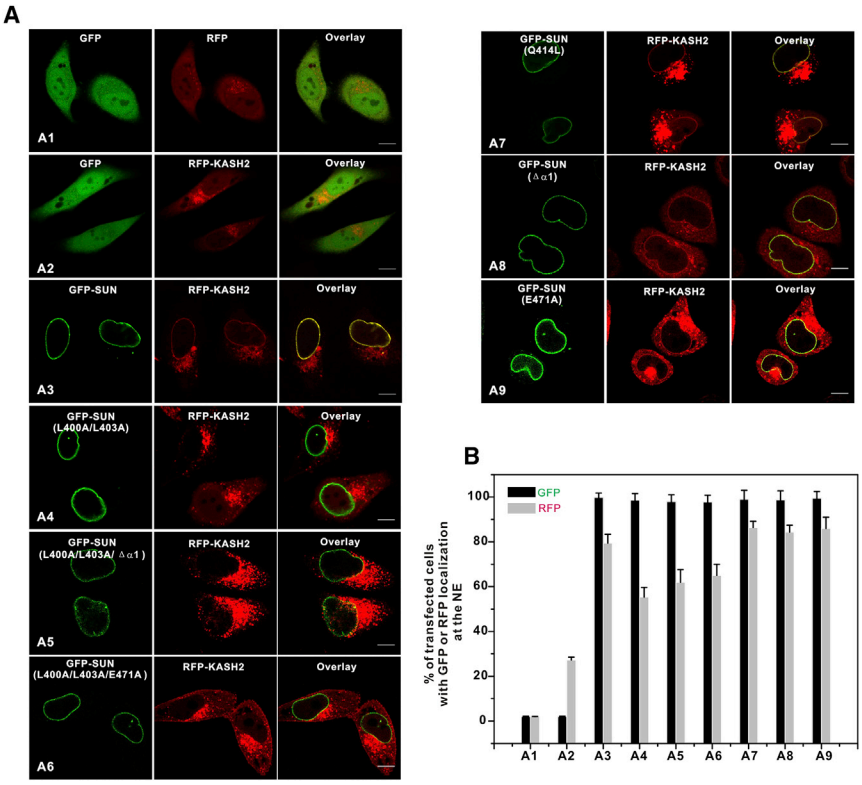

Figure 7. The Coiled-Coil Domains of SUN2 Are Essential for the SUN-KASH Complex Formation

(A) Cellular co-localizations of SUN2 and its mutants with KASH2. GFP and RFP served as the controls, and showed diffused distributions throughout the cytoplasm and nucleus (A1). When overexpressed, a fraction of KASH2 and SUN2 are co-localized at the NE (A3), but GFP alone cannot bring RFP-KASH2 to the NE (A2). In comparison with wild-type SUN2, the Q414L mutant can induce the NE localizations of KASH2 more efficiently (A7), but the L400A/L403A mutant induces less (A4). The mutations (Δα1 and E471A) of CC2 can somewhat rescue the defects caused by the L400A/L403A mutation (A5–A6) and induce more localizations of KASH2 to the NE (A8–A9). Scale bar, 10 μm.

(B) Quantification of the cellular distribution data shown in (A). The percentage of cells showing the NE localization of GFP or RFP was quantified for each construct (average of four experiments, n > 100 cells for each experiment). Each bar represents the mean ± SD.

temperature in thermal denaturation assays (Figure S3). The partially open CC2 three-helix bundle is further completed by the KASH-lid of the SUN domain that inserts into the packing core of the three-helix bundle (Figure 3). Thus, upon dissociation from the SUN domain, the isolated CC2 three-helix bundle might not be well folded but rather could be unstable and flexible. Consistent with this hypothesis, we found that the electron density of CC2 could not be traced in the CC1-CC2 structure while that of CC1 could. Moreover, the intrinsic instability/flexibility of the CC2 three-helix bundle may further implicate that CC2 could be modulated by other unknown factors in SUN domain activation (Figure 3).

CC1-Mediated Trimerization and Activation of the SUN Domain

Distinct from CC2, CC1 of SUN2 adopts a trimeric coiled-coil conformation that would promote SUN domain trimerization (Figure 5). Since CC2-SUN is an inactive monomer and CC1-CC2-SUN forms an active trimer (Figure 1), the CC1-mediated trimerization would also induce some conformational changes of the CC2 three-helix bundle to release the SUN domain for binding to the KASH domain (although the detailed mechanism is unclear at present). Nevertheless, CC1 is most likely the predominant site for regulating the trimerization and activation of the SUN domain based on the structure of the CC1 coiled-coil trimer (Figure 5). However, the structure of the CC1 trimer also revealed a number of unusual structural features that could destabilize the coiled-coil formation, i.e., the hydrophilic residues are located in the inter-helical packing core and there are coiled-coil stacking breaks at the two terminal ends (Figure 6). Due to these structural defects, CC1 is not a perfect coiled coil for trimerization and could be modulated to regulate the oligomeric state and activity of CC1-CC2-SUN. Consistent with this assumption, CC1-CC2-SUN was found to exist in a monomer-trimer equilibrium that could be altered by the mutations in CC1 to stabilize or destabilize the coiled-coil trimer (Figures 6 and S3). More significantly, with the proline-mediated distortion in CC1, the CC1 coiled-coil trimer can transit from the left-handed to the right-handed coiled-coil stacking pattern (Figure 5). In the SUN-KASH complex structure, the helix α3 adopts the right-handed pattern (Figure 4), thus suggesting that the CC1 trimeric coiled-coil could also be further well aligned into the active conformation of the SUN-KASH complex.

Since CC1 is the predominant site for the trimerization and activation of the SUN domain (Figures 1 and 5), the regulation of the CC1 coiled-coil trimer could be a potential mechanism for the control of the SUN-KASH complex formation. Intriguingly, in the structure of the CC1 coiled-coil trimer, a serine (S389) happens to be located in the inter-helical packing interface (Figure 6A) and is predicted to be a phosphorylation site for the kinase PKC (protein kinase C) using NetPhosK (Blom et al., 2004). The phosphorylation of S389 could disrupt the hydrophobic packing core of the coiled-coil trimer, which would lead to the disruption of the SUN-KASH interaction. Moreover, the kinase PKC has also been demonstrated to translocate to the NE under certain stress (Maissel et al., 2006), although the precise function of this kinase in the NE is unclear. Nevertheless, the potential phosphorylation-mediated regulation of CC1 for SUN-KASH complex formation is of interest and awaits further investigation.

Potential Mechanism for the Coiled-Coil-Mediated Regulation of SUN Proteins

Based on the structural studies of the CC2-SUN monomer and the CC1 coiled-coil trimer (Figures 2 and 5), a potential mechanistic model for the coiled-coil-mediated regulation of SUN2

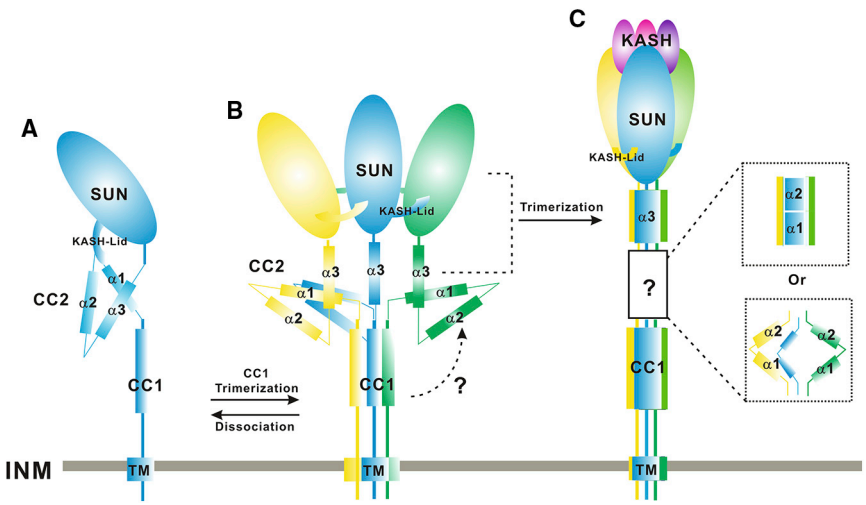

Figure 8. A Schematic Working Model for the Coiled-Coil-Mediated Regulation of SUN2

At the initial stage, CC2 forms a three-helix bundle that could interact with the SUN domain and lock it in an inactive state (A). The CC1-mediated trimerization would likely induce some conformational changes of the CC2 three-helix bundle to release the SUN domain (B). Based on the SUN-KASH complex structure, the SUN domain and α3 of CC2 would work together to form a trimeric conformation for binding to the KASH domain, although it remains to be determined whether the other two helices of CC2 could also form a trimeric coiled coil (highlighted with a question mark) (C). This dynamic process is mediated by CC1 and CC2, and the modulations of these two coiled-coil domains would also likely dictate the overall process.

could be proposed (Figure 8). In this model, CC2 is broken into three short helices and CC1 can form a coiled-coil trimer. At the initial stage, CC2 forms a three-helix bundle that maintains the SUN domain in an inactive conformation (Figure 8A). The CC1-mediated trimerization would somehow induce certain conformational changes of the CC2 three-helix bundle to release the SUN domain (Figure 8B). The competition between the trimeric CC1 coiled coil and the compact CC2-SUN monomer would induce the dynamic monomer-trimer equilibrium of CC1-CC2-SUN. Based on the SUN-KASH complex structure (Figure 4), the SUN domain and α3 of CC2 would work together to form a trimeric conformation for binding to the KASH domain with the help of the CC1 coiled-coil trimer (Figure 8C). However, it remains to be determined whether the other two helices of CC2 could form a trimeric coiled coil as well, or whether they would still remain folded to form a non-coiled-coil trimer (since the reported structure of the SUN-KASH complex is only formed by the minimal truncated fragment of SUN2) (Figure 8C). All of the above processes could be reversed by the destabilization/disruption of the CC1 coiled-coil trimer. Based on similar domain organizations and sequence similarity (Razafsky and Hodzic, 2009; Starr and Fridolfsson, 2010), this proposed internal coiled-coil-mediated regulation of SUN2 could extend to other SUN proteins.

SUN-KASH complexes are essential for the NE organization and a variety of NE-related biological processes (Starr and Fridolfsson, 2010). The assembly and disassembly of SUN-KASH complexes would therefore be in line with the dynamic organization of the NE. For instance, upon cell division in higher eukaryotes, the NE needs to be broken down to expose the chromosomes for segregation; thus, the SUN-KASH complexes embedded in the NE would be also dynamically remodeled (Smoyer and Jaspersen, 2014). However, the simple linear spacer provided by the coiled-coil domains of SUN proteins might not satisfy these complicated processes, which might require the additional regulatory mechanism borne by these coiled-coil domains for controlling SUN-KASH complex formation. Interestingly, recent studies demonstrated that SUN proteins play an active role in NE breakdown and can be modulated to disrupt the interactions with nuclear lamina during mitosis (Patel et al., 2014). Thus, the coiled-coil-mediated dynamic regulation of SUN proteins might also be involved in these biological processes, such as NE organization during cell division.

The finding of coiled-coil-mediated regulation of SUN2 would also broaden the functional versatility of coiled-coil domains. Coiled-coil domains have been traditionally regarded as oligomerization centers for the assembly of supramolecular protein complexes, and often act as the linear spacers to delineate the distance (Gruber and Lupas, 2003; Woolfson et al., 2012). However, accumulating evidence has demonstrated that a large number of coiled-coil domains can exhibit distinct conformations to actively participate in regulating protein activities in addition to oligomerization. For instance, kinesin-3, a family of kinesin motors, contains the non-continuous coiled-coil domains that can fold back to assemble as a bundle-like structure to deactivate the motor domain (Al-Bassam et al., 2003), which is somewhat reminiscent of the negative role of CC2 for the SUN domain of SUN2 (Figure 2). Moreover, the internal coiled-coil domains of myosin VI (a member of myosin motor proteins) even tends to form the single α-helix structure (rather than the coiled-coil dimer) to directly control its walking step sizes (Spink et al., 2008). Thus, together with this study, coiled-coil domains would not simply be linear coiled coils for oligomerization but could be active regulators in controlling a diverse range of biological activities.

EXPERIMENTAL PROCEDURES

Protein Expression and Purification

DNA sequences encoding mouse SUN2 fragments, including CC1 (residues 378–450), CC2 (residues 451–523), CC1-CC2 (residues 378–523), SUN (residues 524–699), CC2-SUN2 (residues 451–699), CC1-CC2-SUN2 (residues 378–699), and various mutants, were each cloned into a modified version of the pET32a vector. Point mutations of CC2-SUN and CC1-CC2-SUN were created using the standard PCR-based mutagenesis method and confirmed by DNA sequencing. Recombinant proteins were expressed in *Escherichia coli* BL21 (DE3) host cells at 16°C. The GB1-His_6-tagged and the Trx-His_6-tagged fusion proteins were purified by Ni^{2+}-Sepharose 6 Fast Flow (GE Healthcare) affinity chromatography followed by SEC (Superdex-200 26/60; GE Healthcare). After cleavage of the tags, the resulting proteins were further purified by another step of SEC with buffer containing 50 mM Tris-HCl (pH 8.0), 100 mM NaCl, 1 mM DTT, 1 mM EDTA. For analytical gel-filtration analysis,

protein samples were concentrated to ~2.5 mg/ml in buffer (50 mM Tris-HCl [pH 8.0], 100 mM NaCl, 1 mM DTT, 1 mM EDTA).

Crystallization, Data Collection, and Structural Determination

Native and selenomethionine (Se-Met) crystals of CC2-SUN (18 mg/ml in 50 mM Tris-HCl [pH 8.0], 100 mM NaCl, 1 mM DTT, 1 mM EDTA), Se-Met crystals of CC1-CC2 (20 mg/ml in 50 mM Tris-HCl [pH 8.0], 100 mM NaCl, 10 mM DTT, 1 mM EDTA) and native crystals of CC1 (20 mg/ml in 50 mM Tris-HCl [pH 8.0], 100 mM NaCl, 1 mM DTT, 1 mM EDTA) were obtained using the sitting-drop vapor diffusion method at 16°C. CC2-SUN was crystallized in 1.4 M Na_2HPO_4/KH_2PO_4 (pH 6.9), while CC1-CC2 and CC1 were crystallized in 0.1 M Tris-HCl (pH 8.0) and 25% (w/v) polyethylene glycol (PEG)3350. The crystals of CC2-SUN were cryo-protected with paraffin oil and 50% (w/v) PEG3350 and the crystals of CC1-CC2 and CC1 were cryo-protected with 25% (w/v) PEG3350, and all the crystals were then flash-frozen by plunging into liquid nitrogen. Diffraction data were collected at the beamline BL17U of the Shanghai Synchrotron Radiation Facility with a wavelength of 0.979 Å at 100 K. For details concerning the structural determination, see Supplemental Experimental Procedures. The protein structure figures were prepared using the program PyMOL (http://www.pymol.org). The statistics for the data collection and structural refinement are summarized in Table 1.

Cell Culture, Imaging, and Data Analysis

DNA sequences encoding full-length SUN2 (wild-type and various mutants) were cloned into pEGFP-C3 vector. The KASH2 fragment (residues 6,799–6,874 of Nesprin-2) was amplified by PCR from Nesprin-2G and cloned into a modified version of pRFP-C1 vector. HeLa cells were cultured in DMEM supplemented with 10% (v/v) fetal bovine serum and grown at 37°C under CO_2 (5%, v/v) for 2–3 days. The cells were transfected with the SUN2 and KASH2 fragments by Lipofectamine 2000 (Invitrogen) according to the manufacturer's instructions. Transfections were normally performed in 12-well plates. In brief, 0.8 μg of GFP-SUN was co-transfected with 0.8 μg of red fluorescent protein (RFP)-KASH2 per well. Fluorescence images were obtained on an Olympus FV1000 laser scanning confocal microscope equipped with a 60× oil-immersion objective lens (numerical aperture = 1.42). Confocal settings used for image capture were held constant in comparison experiments. All fluorescence images were processed and analyzed by ImageJ (NIH). The final quantification graphs were generated by Origin (OriginLab).

Other details can be found in the Supplemental Experimental Procedures.

ACCESSION NUMBERS

The atomic coordinates of the CC2-SUN monomer and the CC1 trimer have been deposited in the PDB with the accession numbers PDB: 5ED8 and 5ED9, respectively.

SUPPLEMENTAL INFORMATION

Supplemental Information includes Supplemental Experimental Procedures and seven figures and can be found with this article online at http://dx.doi.org/10.1016/j.str.2015.10.024.

AUTHOR CONTRIBUTIONS

S.N., H.K., and W.F. conceived and designed experiments; S.N., H.K., F.G., J.R., and M.W. performed the research; L.H. and W.G. gave technical assistance; W.F. coordinated the entire research project and wrote the paper.

ACKNOWLEDGMENTS

We thank the beamline BL17U of the Shanghai Synchrotron Radiation Facility for the beam time. This work was supported by grants from the National Major Basic Research Program of China (2014CB910202 and 2011CB910503) and the National Natural Science Foundation of China (31190062, 31470746, 31300611, and 31200577).

Received: July 28, 2015
Revised: October 21, 2015
Accepted: October 30, 2015
Published: December 10, 2015

REFERENCES

Al-Bassam, J., Cui, Y., Klopfenstein, D., Carragher, B.O., Vale, R.D., and Milligan, R.A. (2003). Distinct conformations of the kinesin Unc104 neck regulate a monomer to dimer motor transition. J. Cell Biol. *163*, 743–753.

Blom, N., Sicheritz-Ponten, T., Gupta, R., Gammeltoft, S., and Brunak, S. (2004). Prediction of post-translational glycosylation and phosphorylation of proteins from the amino acid sequence. Proteomics *4*, 1633–1649.

Brown, J.H., Cohen, C., and Parry, D.A. (1996). Heptad breaks in alpha-helical coiled coils: stutters and stammers. Proteins *26*, 134–145.

Burke, B., and Roux, K.J. (2009). Nuclei take a position: managing nuclear location. Dev. Cell *17*, 587–597.

Cartwright, S., and Karakesisoglou, I. (2014). Nesprins in health and disease. Semin. Cell Dev. Biol. *29*, 169–179.

Chang, W., Worman, H.J., and Gundersen, G.G. (2015). Accessorizing and anchoring the LINC complex for multifunctionality. J. Cell Biol. *208*, 11–22.

Crisp, M., Liu, Q., Roux, K., Rattner, J.B., Shanahan, C., Burke, B., Stahl, P.D., and Hodzic, D. (2006). Coupling of the nucleus and cytoplasm: role of the LINC complex. J. Cell Biol. *172*, 41–53.

Fridkin, A., Penkner, A., Jantsch, V., and Gruenbaum, Y. (2009). SUN-domain and KASH-domain proteins during development, meiosis and disease. Cell. Mol. Life Sci. *66*, 1518–1533.

Gruber, M., and Lupas, A.N. (2003). Historical review: another 50th anniversary—new periodicities in coiled coils. Trends Biochem. Sci. *28*, 679–685.

Gruenbaum, Y., Margalit, A., Goldman, R.D., Shumaker, D.K., and Wilson, K.L. (2005). The nuclear lamina comes of age. Nat. Rev. Mol. Cell Biol. *6*, 21–31.

Haque, F., Lloyd, D.J., Smallwood, D.T., Dent, C.L., Shanahan, C.M., Fry, A.M., Trembath, R.C., and Shackleton, S. (2006). SUN1 interacts with nuclear lamin A and cytoplasmic nesprins to provide a physical connection between the nuclear lamina and the cytoskeleton. Mol. Cell. Biol. *26*, 3738–3751.

Hetzer, M.W. (2010). The nuclear envelope. Cold Spring Harb. Perspect. Biol. *2*, a000539.

Hiraoka, Y., and Dernburg, A.F. (2009). The SUN rises on meiotic chromosome dynamics. Dev. Cell *17*, 598–605.

Kwok, S.C., and Hodges, R.S. (2004). Stabilizing and destabilizing clusters in the hydrophobic core of long two-stranded alpha-helical coiled-coils. J. Biol. Chem. *279*, 21576–21588.

Lupas, A., Van Dyke, M., and Stock, J. (1991). Predicting coiled coils from protein sequences. Science *252*, 1162–1164.

Luxton, G.W., and Starr, D.A. (2014). KASHing up with the nucleus: novel functional roles of KASH proteins at the cytoplasmic surface of the nucleus. Curr. Opin. Cell Biol. *28*, 69–75.

Maissel, A., Marom, M., Shtutman, M., Shahaf, G., and Livneh, E. (2006). PKCeta is localized in the Golgi, ER and nuclear envelope and translocates to the nuclear envelope upon PMA activation and serum-starvation: C1b domain and the pseudosubstrate containing fragment target PKCeta to the Golgi and the nuclear envelope. Cell. Signal. *18*, 1127–1139.

Mejat, A., and Misteli, T. (2010). LINC complexes in health and disease. Nucleus *1*, 40–52.

Mellad, J.A., Warren, D.T., and Shanahan, C.M. (2011). Nesprins LINC the nucleus and cytoskeleton. Curr. Opin. Cell Biol. *23*, 47–54.

Ostlund, C., Folker, E.S., Choi, J.C., Gomes, E.R., Gundersen, G.G., and Worman, H.J. (2009). Dynamics and molecular interactions of linker of nucleoskeleton and cytoskeleton (LINC) complex proteins. J. Cell Sci. *122*, 4099–4108.

Patel, J.T., Bottrill, A., Prosser, S.L., Jayaraman, S., Straatman, K., Fry, A.M., and Shackleton, S. (2014). Mitotic phosphorylation of SUN1 loosens its connection with the nuclear lamina while the LINC complex remains intact. Nucleus *5*, 462–473.

Razafsky, D., and Hodzic, D. (2009). Bringing KASH under the SUN: the many faces of nucleo-cytoskeletal connections. J. Cell Biol. *186*, 461–472.

Schirmer, E.C., Florens, L., Guan, T.L., Yates, J.R., and Gerace, L. (2003). Nuclear membrane proteins with potential disease links found by subtractive proteomics. Science *301*, 1380–1382.

Shimi, T., Butin-Israeli, V., and Goldman, R.D. (2012). The functions of the nuclear envelope in mediating the molecular crosstalk between the nucleus and the cytoplasm. Curr. Opin. Cell Biol. *24*, 71–78.

Smoyer, C.J., and Jaspersen, S.L. (2014). Breaking down the wall: the nuclear envelope during mitosis. Curr. Opin. Cell Biol. *26*, 1–9.

Sosa, B.A., Rothballer, A., Kutay, U., and Schwartz, T.U. (2012). LINC complexes form by binding of three KASH peptides to domain interfaces of trimeric SUN proteins. Cell *149*, 1035–1047.

Sosa, B.A., Kutay, U., and Schwartz, T.U. (2013). Structural insights into LINC complexes. Curr. Opin. Struct. Biol. *23*, 285–291.

Spink, B.J., Sivaramakrishnan, S., Lipfert, J., Doniach, S., and Spudich, J.A. (2008). Long single alpha-helical tail domains bridge the gap between structure and function of myosin VI. Nat. Struct. Mol. Biol. *15*, 591–597.

Starr, D.A., and Fischer, J.A. (2005). KASH 'n Karry: the KASH domain family of cargo-specific cytoskeletal adaptor proteins. Bioessays *27*, 1136–1146.

Starr, D.A., and Fridolfsson, H.N. (2010). Interactions between nuclei and the cytoskeleton are mediated by SUN-KASH nuclear-envelope bridges. Annu. Rev. Cell Dev. Biol. *26*, 421–444.

Stewart-Hutchinson, P.J., Hale, C.M., Wirtz, D., and Hodzic, D. (2008). Structural requirements for the assembly of LINC complexes and their function in cellular mechanical stiffness. Exp. Cell Res. *314*, 1892–1905.

Tapley, E.C., and Starr, D.A. (2013). Connecting the nucleus to the cytoskeleton by SUN-KASH bridges across the nuclear envelope. Curr. Opin. Cell Biol. *25*, 57–62.

Tzur, Y.B., Wilson, K.L., and Gruenbaum, Y. (2006). SUN-domain proteins: 'Velcro' that links the nucleoskeleton to the cytoskeleton. Nat. Rev. Mol. Cell Biol. *7*, 782–788.

Wang, W., Shi, Z., Jiao, S., Chen, C., Wang, H., Liu, G., Wang, Q., Zhao, Y., Greene, M.I., and Zhou, Z. (2012). Structural insights into SUN-KASH complexes across the nuclear envelope. Cell Res. *22*, 1440–1452.

Wilhelmsen, K., Ketema, M., Truong, H., and Sonnenberg, A. (2006). KASH-domain proteins in nuclear migration, anchorage and other processes. J. Cell Sci. *119*, 5021–5029.

Wilson, K.L., and Berk, J.M. (2010). The nuclear envelope at a glance. J. Cell Sci. *123*, 1973–1978.

Woolfson, D.N., Bartlett, G.J., Bruning, M., and Thomson, A.R. (2012). New currency for old rope: from coiled-coil assemblies to alpha-helical barrels. Curr. Opin. Struct. Biol. *22*, 432–441.

Zhou, K., and Hanna-Rose, W. (2010). Movers and shakers or anchored: *Caenorhabditis elegans* nuclei achieve it with KASH/SUN. Dev. Dyn. *239*, 1352–1364.

Zhou, Z., Du, X., Cai, Z., Song, X., Zhang, H., Mizuno, T., Suzuki, E., Yee, M.R., Berezov, A., Murali, R., et al. (2012). Structure of Sad1-UNC84 homology (SUN) domain defines features of molecular bridge in nuclear envelope. J. Biol. Chem. *287*, 5317–5326.